



说明

各种各样的应用利用飞行时间 (ToF) 光学方法以高精度测量距离，这些应用包括激光安全扫描仪、测距仪、无人机、制导和自动驾驶系统等。该参考设计详述了基于高速数据转换器的解决方案的优点，包括目标识别、宽松的采样率要求和简化的信号链。该设计还解决了光学器件、驱动器和接收器前端电路、模数转换器 (ADC)、数模转换器 (DAC) 和信号处理问题。

资源

TIDA-01187	设计文件夹
ADC3244	产品文件夹
DAC5682Z	产品文件夹
OPA695	产品文件夹
OPA857	产品文件夹
THS4541	产品文件夹
CDCM7005	产品文件夹



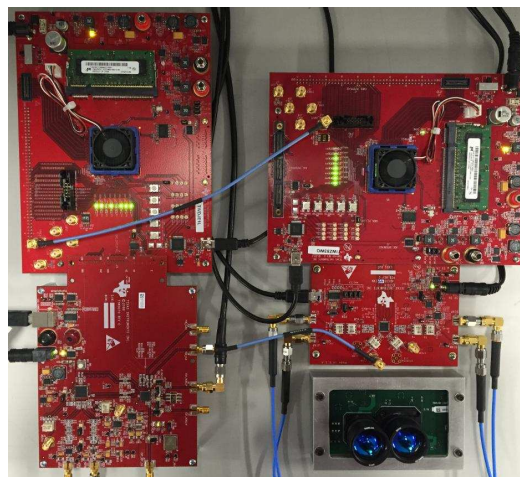
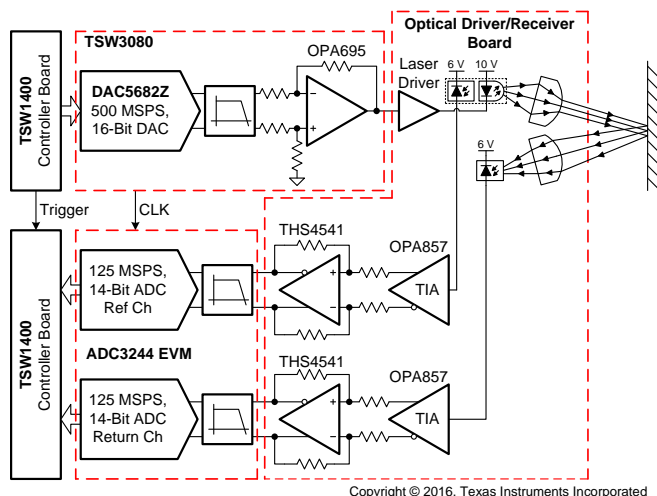
咨询我们的 E2E 专家

特性

- 采用额外的光学器件和激光能量，测量距离高达 9m 或更远
- 距离测量平均误差小于 $\pm 6\text{mm}$ ，标准偏差小于 3cm
- 5.75W 脉冲 905nm 近红外线激光二极管和驱动器，平均输出功率小于 1mW
- 近红外线 PIN 光电二极管高速互阻抗放大器前端
- 激光准直和光接收器聚焦光学器件
- 包括 14 位 125MSPS ADC 和 16 位 500MSPS DAC 高速放大器和时钟
- 具有基于 DFT 的距离估算功能的脉冲 ToF 测量方法
- 为选定的器件提供了汽车级版本

应用

- 架构测量设备
- 汽车扫描 LIDAR
- 无人机
- 气体分析
- 激光测距仪 (LIDAR)
- 激光安全扫描仪
- 视网膜成像
- 机器人





该 TI 参考设计末尾的重要声明表述了授权使用、知识产权问题和其他重要的免责声明和信息。

1 System Description

The coherent nature of light emitted from a laser makes it especially useful in the measurement of distance because it can be easily collimated into a narrow beam with minimal divergence. The constant speed of light at approximately 3×10^8 m/s can be used to estimate distance by measuring the time it takes for the emitted light of a laser to travel to the target and back. Small laser and photo diodes have made it possible to build compact and portable systems, which enable applications including laser safety scanners, drones, laser range finders and guidance systems.

1.1 Key System Specifications

表 1. Key System Specifications

PARAMETER	SPECIFICATIONS	DETAILS
Range	1.5 m to 9 m	3.5 节
Range measurement standard deviation	< 1 cm at 5 m, < 3 cm at 9 m	3.5 节
Range measurement mean error	< ± 6 mm	3.5 节
Laser peak power	5.75 W	节 2.3.6.3
Laser average power	< 1 mW	节 2.3.6.3
Wavelength	905 nm	3.3 节

2 System Overview

图 1 shows a simplified diagram of a laser-based distance measurement system. In this system, light emitted by the laser is first collimated by a lens to create a narrow beam, which then travels down range and after reflecting off the target returns back to be focused on the detector by a second lens. The laser driver and stimulus subsystem can be designed to apply pulsed or amplitude modulation (AM) waveforms. Some lasers are capable of frequency modulation (FM) (that is, modulation of the emitted wavelength), but they are beyond the scope of this design.

The optical detector is typically a PIN or avalanche photo diode, which produces a small current proportional the return signal. A very-low-noise transimpedance amplifier (TIA) is required to optimize the range of the system because the amplitude of the return signals decreases proportionally to the square of the distance. The amplified return signal is measured and processed to produce a range measurement. The optics used in this design are optimized for up to 9 m of distance. A longer range is possible through a choice of optics.

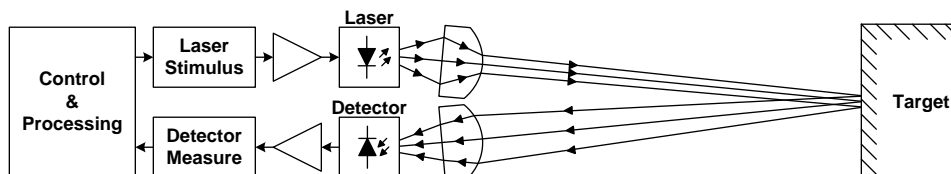
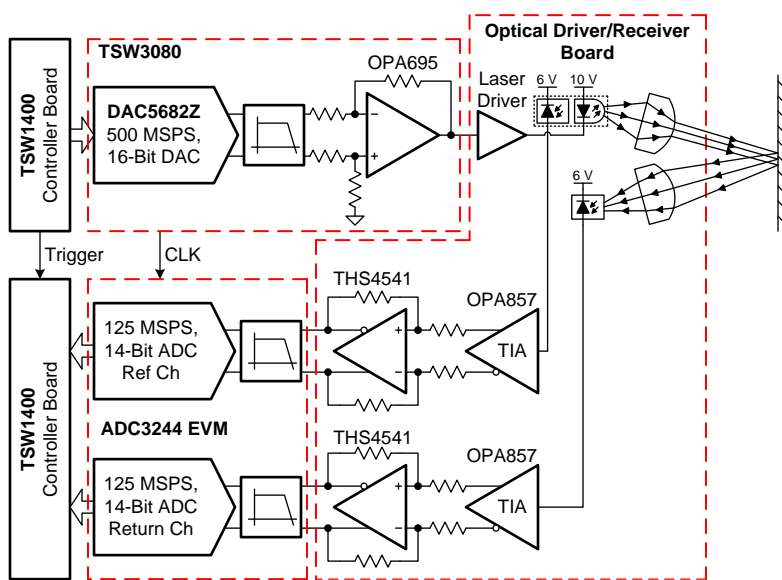


图 1. Simplified System Diagram

This design highlights the advantages of a high-speed ADC or DAC based signal chain for laser distance measurement systems. The guide also describes a pulsed ToF-based system using phase-shift based range estimation.

2.1 Block Diagram

This design comprises five circuit boards that work together to form a system for laser distance measurement.



Copyright © 2016, Texas Instruments Incorporated

图 2. Block Diagram

2.1.1 Optical Driver and Receiver Board

This board contains the laser driver, near infrared (NIR) laser diode, laser collimating lens, receiver focusing lens, PIN receiver and reference photo diodes, and corresponding TIAs. Laser driver stimulus input from the DAC evaluation module (EVM) and TIA received output from the TIAs to the ADC EVM is provided through SMP coax connectors. The optics are off-the-shelf components available from Thorlabs.

2.1.2 TSW3080 Board

This board provides the laser driver stimulus and is based on the DAC5682Z 1-GSPS DAC and OPA695 high-speed operational amplifier (op amp). The DAC is operated at 500 MSPS with no interpolation. A divide-by-4 version of the DAC clock is connected to the ADC EVMs clock input so that the boards sample coherently with respect to each other. A RF signal generator is used to provide a 1-GHz clock for the system.

2.1.3 ADC3244 EVM

The EVM for the ADC3244 provides a dual-channel, 14-bit, 125-MSPS ADC used to capture input from both the reference TIA and return signal TIA. These inputs are bandwidth limited to 40 MHz by the boards low-pass filters.

2.1.4 TSW1400 Controller Board

Two TSW1400 controller boards are used in the system. The first board is used to drive the stimulus signal into the DAC while the other board captures the output of the reference and return signal channels. The triggering features of these boards are utilized to create a synchronized capture between the DAC and the ADC.

2.2 Highlighted Products

2.2.1 ADC3244

The ADC3244 is a high-linearity, ultra-low-power, dual-channel, 14-bit, 125-MSPS, ADC with a serial low-voltage differential signaling (LVDS) to reduce the number of interface lines. The serial LVDS interface is two-wire, where each ADC data are serialized and output over two LVDS pairs. An internal phase-locked loop (PLL) multiplies the incoming ADC sampling clock to derive the bit clock that is used to serialize the 14-bit output data from each channel. In addition to the serial data streams, the frame and bit clocks are also transmitted as LVDS outputs. The ADC3244 is available in a VQFN-48 package (7 mm × 7 mm).

2.2.2 DAC5682Z

The DAC5682Z is a dual-channel, 16-bit, 1-GSPS DAC with wideband LVDS data input, integrated 2×/4× interpolation filters, onboard clock multiplier, internal voltage reference and a wideband LVDS port with on-chip termination. Full-rate input data can be transferred to a single DAC channel, or ½-rate and ¼-rate input data can be interpolated by onboard 2×- or 4×-FIR filters. An on-chip delay lock loop (DLL) simplifies LVDS interfacing by providing skew control for the LVDS input data clock. The DAC5682Z is available in a QFN-64 package (9 mm × 9 mm).

2.2.3 OPA695

The OPA695 is a 1400-MHz bandwidth (gain = 2 V/V), current-feedback op amp that combines an exceptional 4300-V/ μ s slew rate and low input voltage noise. The device is available in SOIC-8, VSSOP-8, and SOT23-6 packages.

2.2.4 OPA857

The OPA857 is a wideband, fast overdrive recovery, fast-settling, ultra-low-noise TIA that targets photodiode monitoring applications. With selectable feedback resistance, the OPA857 simplifies the design of high-performance optical systems. Very-fast overload recovery time and internal input protection provide the best combination to protect the remainder of the signal chain from overdrive while minimizing recovery time. The two selectable transimpedance gain configurations allow the high dynamic range and flexibility required in modern TIA applications. The OPA857 is available in a VQFN (3 mm \times 3 mm) package.

2.2.5 THS4541

The THS4541 is a low-power, voltage-feedback, fully differential amplifier (FDA) with an input common-mode range below the negative rail and rail-to-rail output. The device has a 1500-V/ μ s slew rate, a 500-MHz bandwidth (gain = 2 V/V) and is available in VQFN-16 (3 mm \times 3 mm) and WQFN-10 (2 mm \times 2 mm) packages.

2.2.6 CDCM7005

The CDCM7005 is a high-performance, low-phase-noise and low-skew clock synchronizer that synchronizes a VCXO or VCO frequency to one of the two reference clocks. The programmable pre-divider M and the feedback-dividers N and P give high flexibility to the frequency ratio of the reference clock to VCXO. The outputs are user definable to LVCMOS or LVPECL. This device is available in a 48-pin VQFN (7 mm \times 7 mm) or a 64-pin BGA (8 mm \times 8 mm).

2.3 System Design Theory

2.3.1 Pulsed ToF Method Overview

The most direct way to estimate distance using the system mentioned in the previous sections is to apply a short duration pulse to the laser and measure the time from when the pulse of light is emitted until it returns to the detector. ToF can be measured using a time-to-digital converter (TDC) or a high-speed ADC and the resulting distance can be calculated using the following 公式 1. The TDC operates like a high-speed stopwatch directly counting time between start and stop events, while the ADC measures the return signal at a regular interval, which is then processed to estimate time. As 公式 1 shows, because of the high speed of light, small amounts of time equate to substantial distances. For instance, ± 1 ns of error in the measurement of time results in ± 15 cm of distance estimation error. The range estimation performance of pulsed ToF measurement is therefore directly proportional to the ability of the system to measure small time intervals.

$$d = \frac{c \times t}{2}$$

where

- d is the distance in meters
- c is the speed of light in air (3×10^8 m/s)
- t is the ToF in seconds (laser to target and back to detector)

(1)

Range resolution is inversely proportional to the combined rise time of the laser, TIA and detector, while the maximum range is proportional to peak laser power and the combined sensitivity of the TIA and detector for the given optics. This indicates that to achieve high resolution over long distances, the system should have a high-peak-power laser with a fast rise time measured by a high bandwidth, low-noise photo diode, TIA, and detector. Additionally, the system must account for the return signal amplitude, which decreases proportionally to the square of the measured distance. The finite rise time of the measured return must also be accounted for in the detector to prevent level-dependent triggering errors.

TDC-based systems must solve the previously mentioned problems directly in the analog domain, which implies that fast rise time pulses and high receive bandwidth are required. The receive path also generally requires automatic gain control (AGC) to account for the return signal level and a time discriminator to ensure triggering occurs at a constant point in the rise of the return signal.

A high-speed ADC based system has a number of performance advantages over those based on a TDC. Because the ADC digitizes the return signal (instead of simply measuring time), signal processing can be employed to implement sophisticated detection schemes that not only have better performance than the TDC, but also provide additional information for target identification. This result allows for the relaxation of the laser rise time or improvement in range resolution for the same rise time. The wide dynamic range of the ADC eases and in some systems even eliminates the requirement for AGC in the receive path.

2.3.2 Phase-Shift Method Overview

An alternative to pulsed ToF is the phase shift ToF method, where the laser output power is AM modulated with a continuous wave (CW) signal. The phase difference between the transmitted and received signal is measured and distance is estimated using 公式 2. As with pulsed ToF measurements, the range resolution is directly proportional to the CW stimulus frequency if the phase error tolerance has been held constant. The repetitive nature of a CW signal creates the potential for aliasing if the distance exceeds the maximum unambiguous range described by 公式 3, which creates a tradeoff between range and resolution. This problem can be mitigated by using two different CW frequencies, one of lower frequency that provides range and the other of higher frequency that provides resolution.

$$d = \frac{c \times \Theta}{4 \times \pi \times f}$$

where

- d is the distance in meters
- c is the speed of light in air (3×10^8 m/s)
- θ is the phase angle in radians between the transmitted and received signals
- f is the frequency of the CW of the transmitted signal

(2)

$$r = \frac{c}{2 \times f}$$

where

- r is the maximum unambiguous distance in meters
- c is the speed of light in air (3×10^8 m/s)
- f is the frequency of the CW of the transmitted signal

(3)

The measuring phase can be accomplished a number of ways including the use of a heterodyne receiver and a high-speed ADC. With the heterodyne receiver method, a local oscillator (LO) is mixed with both the transmitted CW and the received return signal. The phase difference between these two intermediate frequencies (IFs) can be measured with low-speed ADCs. Direct sampling of the return signal with a high-speed ADC has a number of significant advantages over the heterodyne receiver. Firstly, the broadband

nature of high-speed ADCs allows the simultaneous reception of multiple CW frequencies so that both range and resolution can be achieved at the same time. Removing the LO generator, mixers, and bandpass filters required with the heterodyne receiver not only reduces the cost and complexity of the system, but also eliminates the performance limitations that RF receivers experience, such as receiver linearity, transmitter and receiver crosstalk, and dynamic range. As with the pulsed ToF method, the high-speed ADC generally also eliminates much of the requirement for AGC and makes target detection more straightforward.

2.3.3 Overview of Pulsed ToF With Phase-Shift-Based Estimation Method

This design uses a pulsed ToF stimulus with a phase shift range estimation algorithm based on a high-speed ADC signal chain. Pulsed ToF has the advantage of producing high peak, but low average optical power, which is important for systems that must adhere to eye safety requirements. A pulsed laser driver is also generally more straightforward to implement, which results in reduced system complexity and cost. The discrete Fourier transform (DFT) is used to estimate the phase of both the reference and return signals, the delta of which can be used to calculate distance as with the phase shift method (using [公式 2](#)).

[图 3](#) shows the stimulus used, where N narrow pulses are transmitted in each frame and the return and reference signal are both coherently digitized with a capture synchronized to the transmitter. A subset of the digitized samples equivalent to exactly N periods are selected for processing (see [图 4](#)). The sample window is chosen in such a way to include all N periods of the reference and return signal. This implies a maximum ambiguous range as noted with the phase shift method that must be accounted for, which can be controlled by setting the period of the pulses.

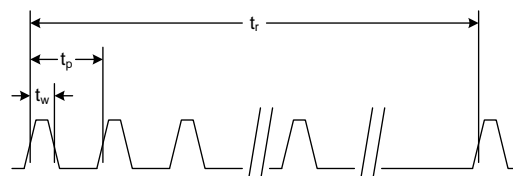


图 3. Laser Stimulus Waveform

The pulse width, t_w , is selected to be just wide enough that the pulse can be sampled with a few samples. The pulse period, t_p should be selected such that both the maximum unambiguous distance requirement is met and the filtered TIA output has time to settle. The number of pulses per frame impacts the standard deviation of the measurement. Increasing the number of pulses reduces the standard deviation and the expense of higher average power. The variable t_r sets both the frame rate and average power of the laser.

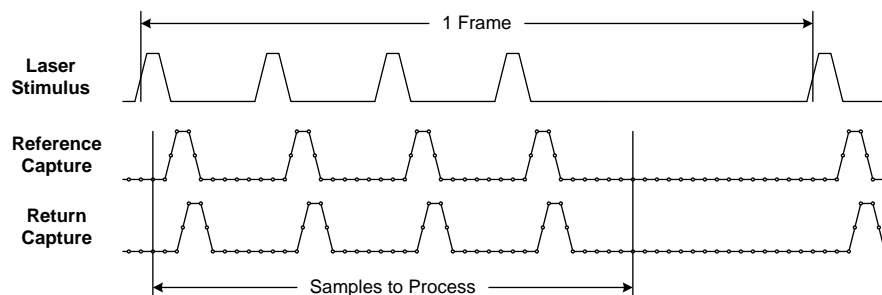


图 4. Captured Reference and Return Waveforms

The return and reference sample set are processed using a non-windowed DFT. The phase of the fundamental or one of the harmonics of the reference is then subtracted from that of the return. This is then converted to distance using 公式 2 and scaled for gain and offset based on calibration data (see 图 5).

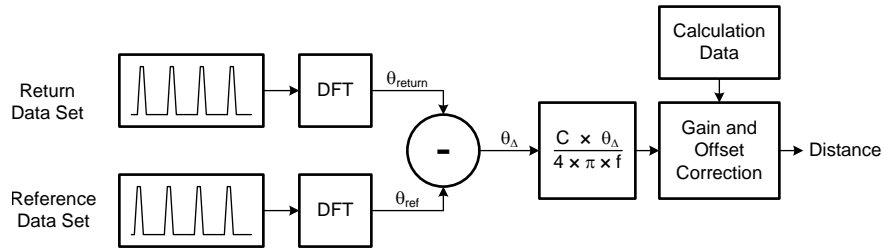


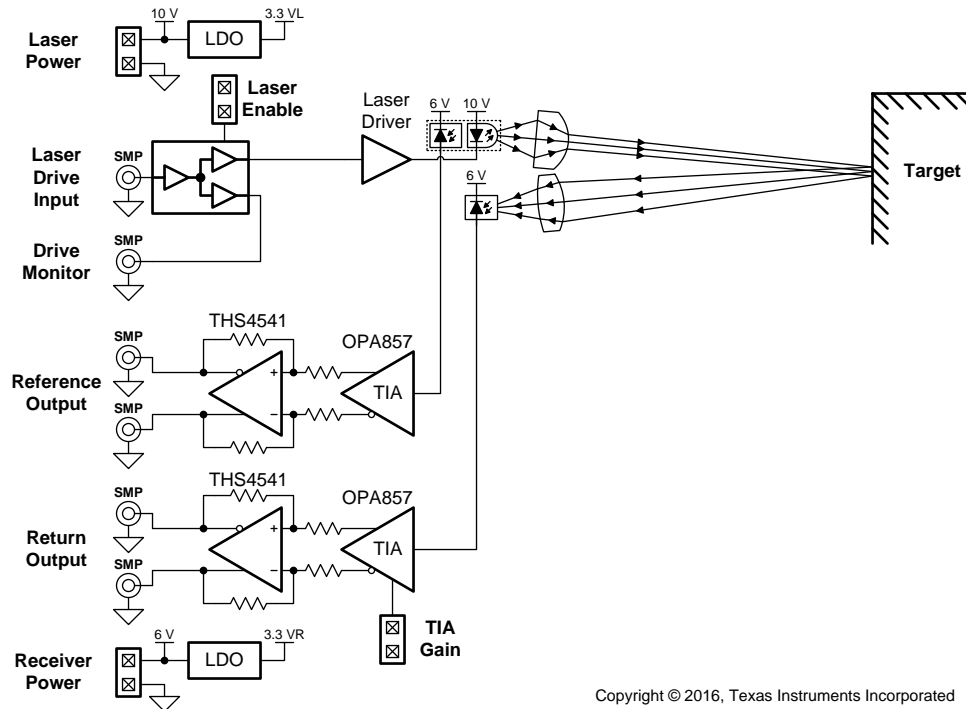
图 5. Distance Calculation Algorithm

For this design, pulse width, t_w , has been set to 30 ns, which results in about seven ADC samples per pulse after filtering. A period, t_p , has been set to 512 ns to ensure that the filtered TIA output settles between pulses and ten pulses transmitted per frame. The frame has been set to 2 ms so that the average laser power is less than 1 mW. For each measured frame, 640 samples are taken for the capture after the trigger. After taking the DFT, the phase in Fourier bin 20 (which corresponds to the second harmonic of the pulse train) is taken for both reference and return and then processed with gain and offset correction to produce a distance measurement. The second harmonic was selected because it showed the lowest mean range error and standard deviation for this design.

2.3.4 System Construction

2.3.4.1 Optical Driver and Receiver Board

图 6 显示的是光学驱动器和接收器板的块图，该板包括激光驱动器、激光二极管、准直和聚焦光学元件，以及参考和返回光电二极管接收电路。该板由 6-V 电源为光电二极管接收电路供电，并由 10-V 电源为激光驱动器电路供电，每个电源都有 3.3-V 电压调节器用于电路的低电压部分。SMP 同轴连接器用于将输入和输出连接到系统中的其他板。



Copyright © 2016, Texas Instruments Incorporated

图 6. Optical Driver and Receiver Board Block Diagram

图 7 显示了光学驱动器和接收器板的前面，该板容纳了激光二极管和参考和返回光电二极管。准直和聚焦光学元件通过镜头管安装法兰连接到板。

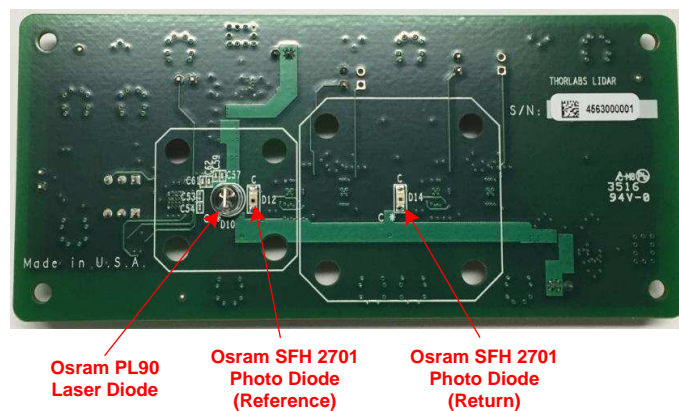


图 7. Optical Driver and Receiver PCB—Front View

图 8 shows the back side of the board, which houses all of the active circuitry. The *TIA Gain* for the return channel and *Laser Enable* are controlled through jumpers.

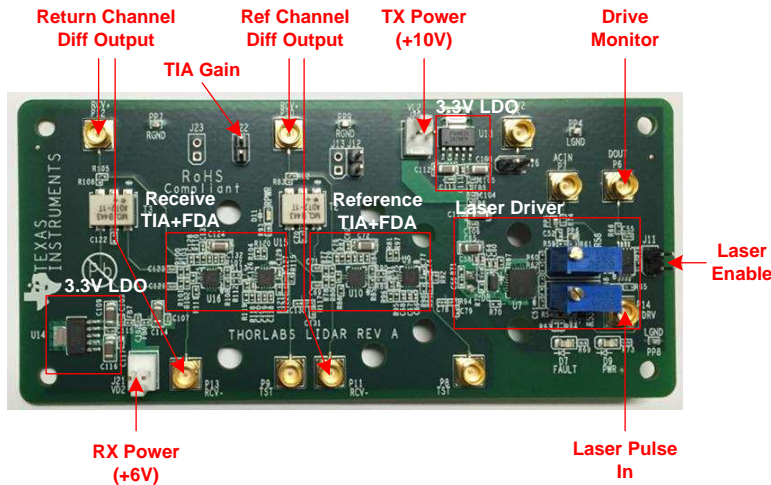


图 8. Optical Driver and Receiver PCB—Back View

2.3.4.2 DAC Source and ADC Capture Board Setup

图 9 shows the setup TSW3070 (DAC5682Z), ADC3244 EVM and two TSW1400 controller boards. Each board has a USB and DC wall-adapter power connection. Additionally, the SYNC output of the DAC TSW1400 is connected to the TRIGGER input of the ADC TSW1400 through an SMA coax cable, which synchronizes the source and capture. The 125-MHz CLK output of the TSW3070 drives the clock input of the ADC3244 EVM through an SMA coax cable. The TSW3070 receives a 15-dBm, 1-GHz clock input from a RF signal generator through an SMA coax cable.

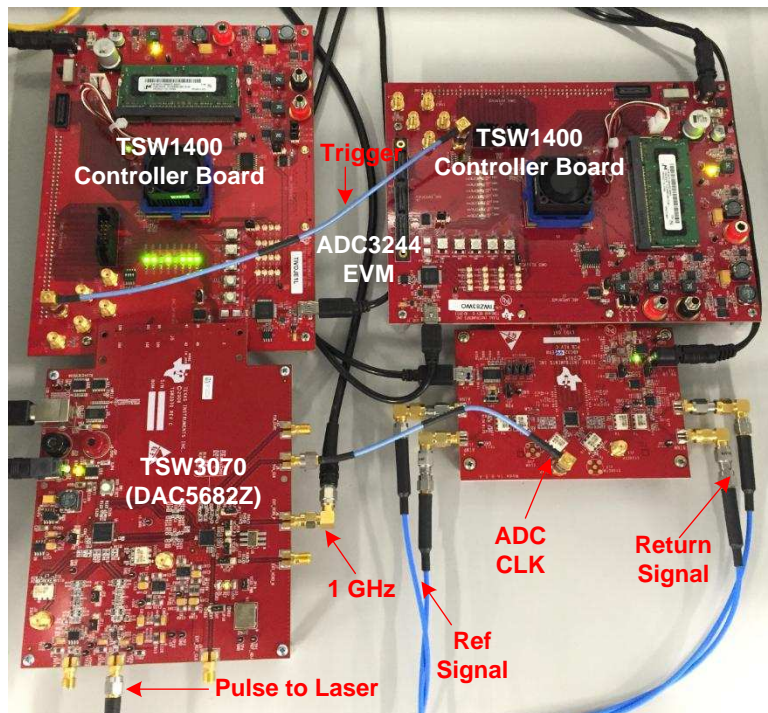


图 9. DAC Source and ADC Capture Board Setup

The DAC output of the TSW3070 and reference and return differential inputs to the ADC3244 connect to the optical driver and receiver board through SMA-to-SMP coax cables.

2.3.5 Optics

This design uses off-the-shelf optics and mounting components from Thorlabs to demonstrate collimation of the laser and focusing of the return signal onto the photodiode. 图 10 shows a cross section of the optics along with the laser diode and photodiodes. These components have been selected to balance a number of design objectives while retaining a straightforward implementation. The laser driver and reference and return receivers have been implemented on a single printed-circuit board (PCB) with optics attached through flanges.

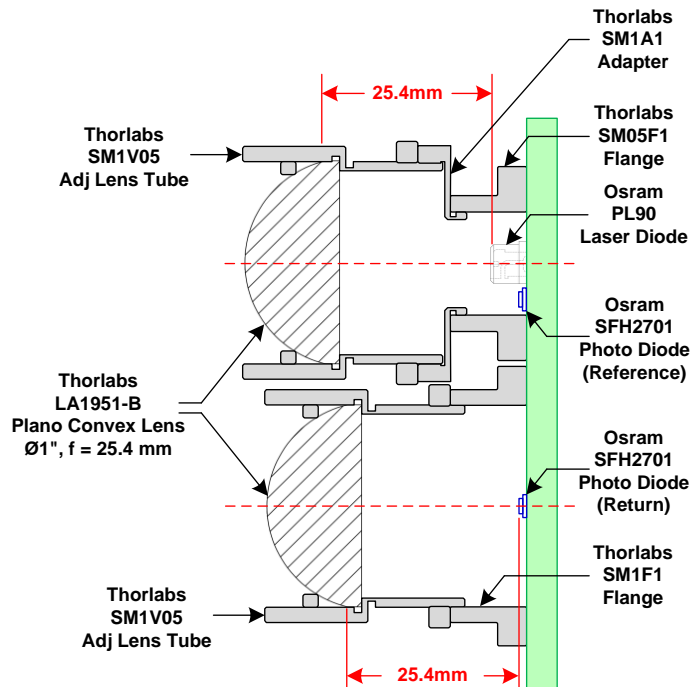


图 10. Cross Section of Optics

A 0.5-in flange (SM05F1) is used along with a 0.5-in to 1.0-in adapter (SM1A1) for the laser optics so that the laser and receiver lens tubes can be mounted as close together as possible. This is important because it determines the minimum range where the field of view (FOV) of the receiver includes the laser beam. Both driver and receiver optics use adjustable lens tubes with locking rings (SM1V05), which makes collimation of the laser and focusing of the return straightforward. The holes in the PCB for the flanges are drilled oversized to facilitate alignment.

2.3.5.1 Collimating Lens

Laser diodes typically produce highly divergent light, which is not very useful for distance measurement applications. The process of collimation takes the fan of light rays from the laser diode emitter and straightens them out into a narrow beam. Because the laser has an emitter with a finite aperture size (that is, it is not a perfect point source), some residual divergence remains after collimation. 图 11 shows the collimation process and 公式 4 and 公式 5 show the trade-off between beam width and divergence for a given emitter aperture size.

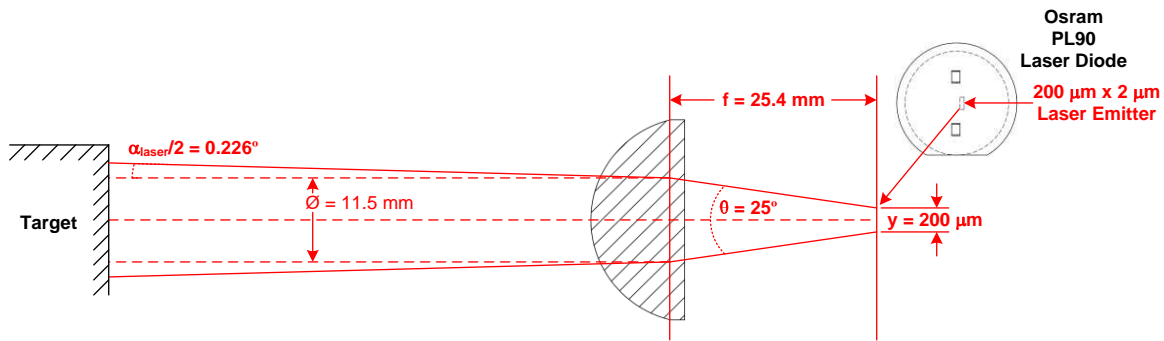


图 11. Collimation of Beam

$$\varnothing_{\text{laser}} = 2 \times f \times \text{TAN}\left(\frac{\theta}{2}\right) + y$$

where

- $\varnothing_{\text{laser}}$ is the beam width in mm
- f is the focal length in mm
- θ is the beam laser divergence angle in $^{\circ}$
- y is the laser emitter aperture length in mm

(4)

$$\alpha_{\text{laser}} = 2 \times \text{ATAN}\left(\frac{y}{2 \times f}\right)$$

where

- α_{laser} is the beam divergence angle in $^{\circ}$
- y is the laser emitter aperture length in mm
- f is the focal length in mm

(5)

The OSRAM PL90 laser diode has been selected for its ability to generate high-peak-power pulses with a fast rise time. This laser diode has an aperture of $200 \mu\text{m} \times 2 \mu\text{m}$ with a divergence angle of 8° parallel to the emitter and 25° perpendicular to the emitter. For beam width and divergence calculations, the longer of the two aperture dimensions ($200 \mu\text{m}$) and the larger of the two divergence angles (25°) are used for y and θ respectively.

A Thorlabs LA1951-B 1-in diameter Plano-Convex lens with a 25.4-mm focal length has been selected to collimate the laser. This focal length balances beam width and divergence angle given the relatively large emitter width of $200 \mu\text{m}$ and the desire to keep the distance between the laser and receiving photodiode as small as possible. The Plano-Convex lens profile is commonly used for collimation and has been selected over more expensive spherical and best form profiles because they did not offer any significant advantages. The lens has an anti-reflective coating appropriate for 905-nm operation which improves the optical output of the collimated beam.

Using this setup, a beam width of 11.5 mm with a divergence angle of 0.226° has been achieved. At 9 m, this yields a beam width of about 82.5 mm, which is still quite usable for ranging. Increasing focal length lessens the spreading of the beam because of divergence, but increases the beam diameter. The usable aperture of the Plano-Convex lens is about 90% of its diameter, which implies that the focal length could be increased to approximately 50 mm with a beam width of 22.4 mm.

图 12 shows a cross section of the collimating optics setup. The alignment process involves adjusting both the placement of the SM05F1 mounting flange and lens focus through the SM1V05 adjustable lens tube. Because the output of the laser diode is invisible near infrared light, a Thorlabs VRC4 detector card is used to make the beam visible during the alignment process. This card has a photosensitive coating which emits green light when illuminated by the laser.

Because the laser aperture has a wide aspect ratio (200 μm \times 2 μm), the collimated beam results in a thin rectangle instead of a round spot. The lens focus is adjusted until a small rectangle is visible on the detector card that diverges minimally as the range increases. When the beam is roughly collimated, the flange position is adjusted such that the beam is focused on the center of the target.

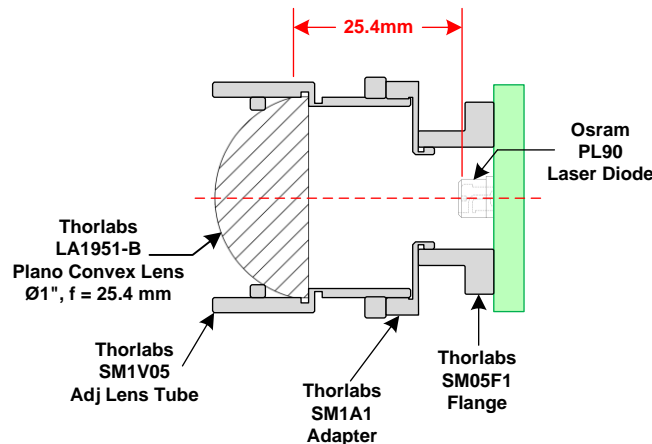


图 12. Collimating Optics Cross Section

2.3.5.2 Focusing Lens

Light returning from the target is focused by a Thorlabs LA1951-B 1-in diameter Plano-Convex lens onto a OSRAM SFH2701 PIN photodiode using an assembly that 图 13 shows. The diameter of the focusing lens determines its light-collecting ability, while focal length sets the FOV. Placing the laser close to the receiver is desirable so that its FOV includes that of the laser at close range; however, there is a trade-off between light-collecting ability and close range capability. To further improve the light-collecting capability, a lens with an anti-reflective coating active in the NIR region has been selected.

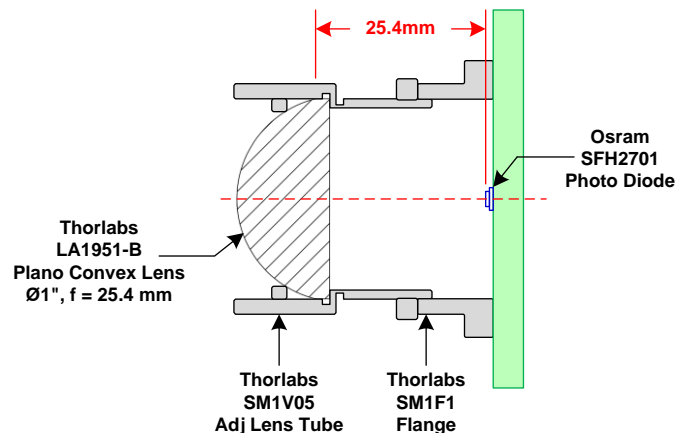


图 13. Focusing Optics Cross Section

The OSRAM photodiode used for this design has an active detecting region of $600\ \mu\text{m} \times 600\ \mu\text{m}$. To maximize the received signal, the lens is aligned and focused to a spot size that just covers all of the active region of the detector, which yields a diameter of approximately $\sqrt{2} \times 600\ \mu\text{m} = 850\ \mu\text{m}$. When combined with the focal length of the lens, a FOV can be determined by using 图 14. The FOV angle is chosen to be larger than the divergence angle of the laser (0.452°) so that all of the return light can be collected. With a 25.4-mm focal length and spot size of $850\ \mu\text{m}$, a FOV angle of 1.92° is achieved. This angle is significantly larger than that of the laser, which eases focusing and alignment while delivering the ability to operate at ranges less than 2 m.

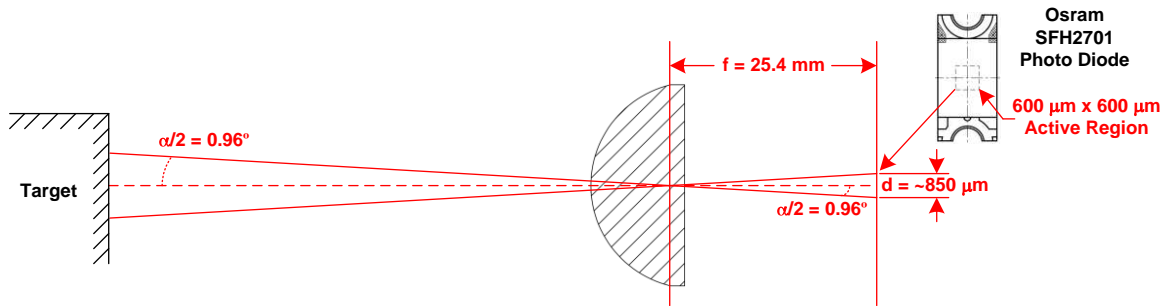


图 14. Receiver Field of View

$$\alpha = 2 \times \text{ATAN}\left(\frac{d}{2 \times f}\right)$$

where

- α is the FOV in $^\circ$
- d is the diameter of a circle incorporating the active region of the photodiode in mm
- f is the focal length in mm

(6)

A number of lens profiles are appropriate for focusing, including Plano-Convex, best form and spherical. The Plano-Convex is the most economical lens profile and the improved spherical aberration performance of best form profile and shorter possible focal length of spherical profiles did not offer improvements for this application. If outdoor operation is desired, an optical filter can be added to the receive lens tube to reduce the impact of sunlight.

2.3.6 Laser Transmit Path

2.3.6.1 High-Speed Transmit Signal Chain

The DAC5682Z is operated at 500 MSPS with no interpolation. A 1-GHz signal generator drives the CDCM7005 clock synchronizer and PLL, which is used as a clock divider to produce all the clocks for the system. As 图 15 shows, the DAC receives 500 MHz (divide-by-2), the ADC receives 125 MHz (divide-by-8), and the TSW1400 receives 250 MHz (divide-by-4). The clock for the ADC EVM is taken from the TSW3080 clock output.

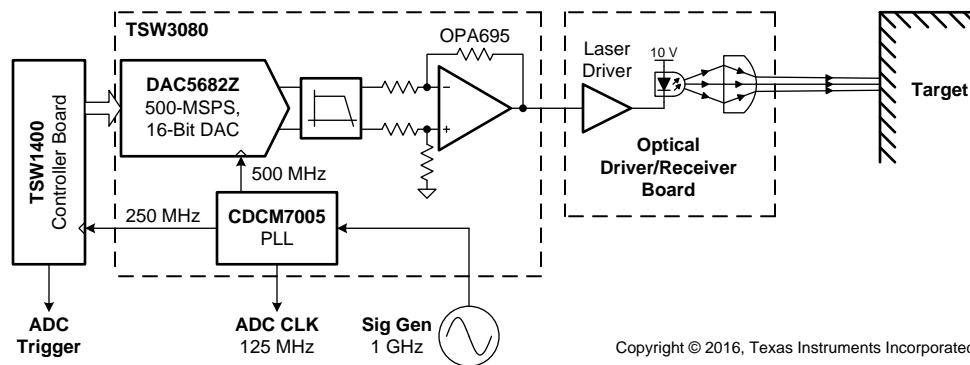
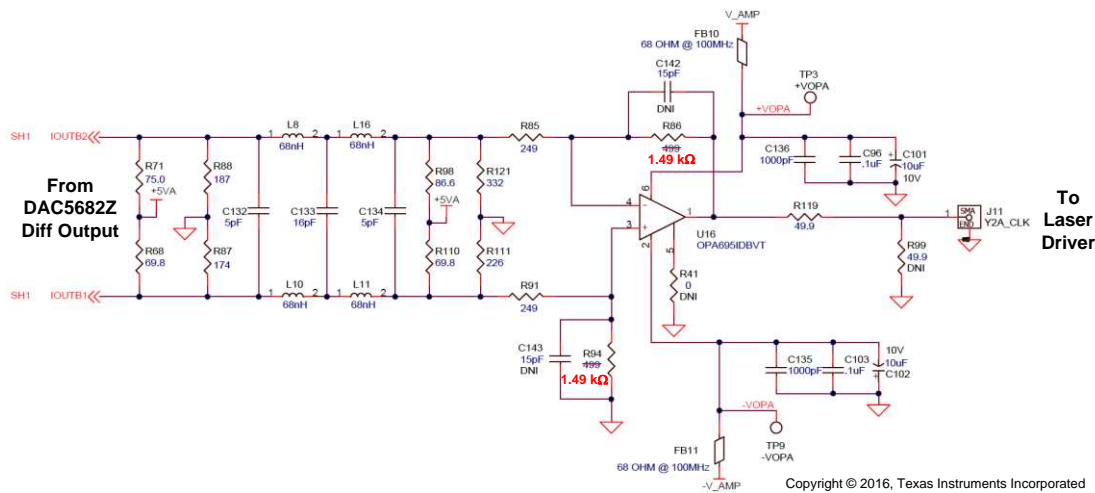


图 15. HS Transmit Signal Chain

The TSW1400 controller board is used to provide stimulus to the DAC through a waveform stored in its memory. This waveform is looped continuously with a trigger being generated at the beginning of each cycle, which is sent to the second TSW1400 used for capturing the ADC results. The output of the DAC is low-pass filtered before being converted into a voltage by the OPA695 high-speed op amp. This signal is driven through a coax cable to the optical driver and receiver board, where it is connected to the laser driver input. The laser driver applies current pulses into the laser, which is then collimated and aligned with the target.

2.3.6.2 High-Speed DAC Antialiasing and I-V Conversion

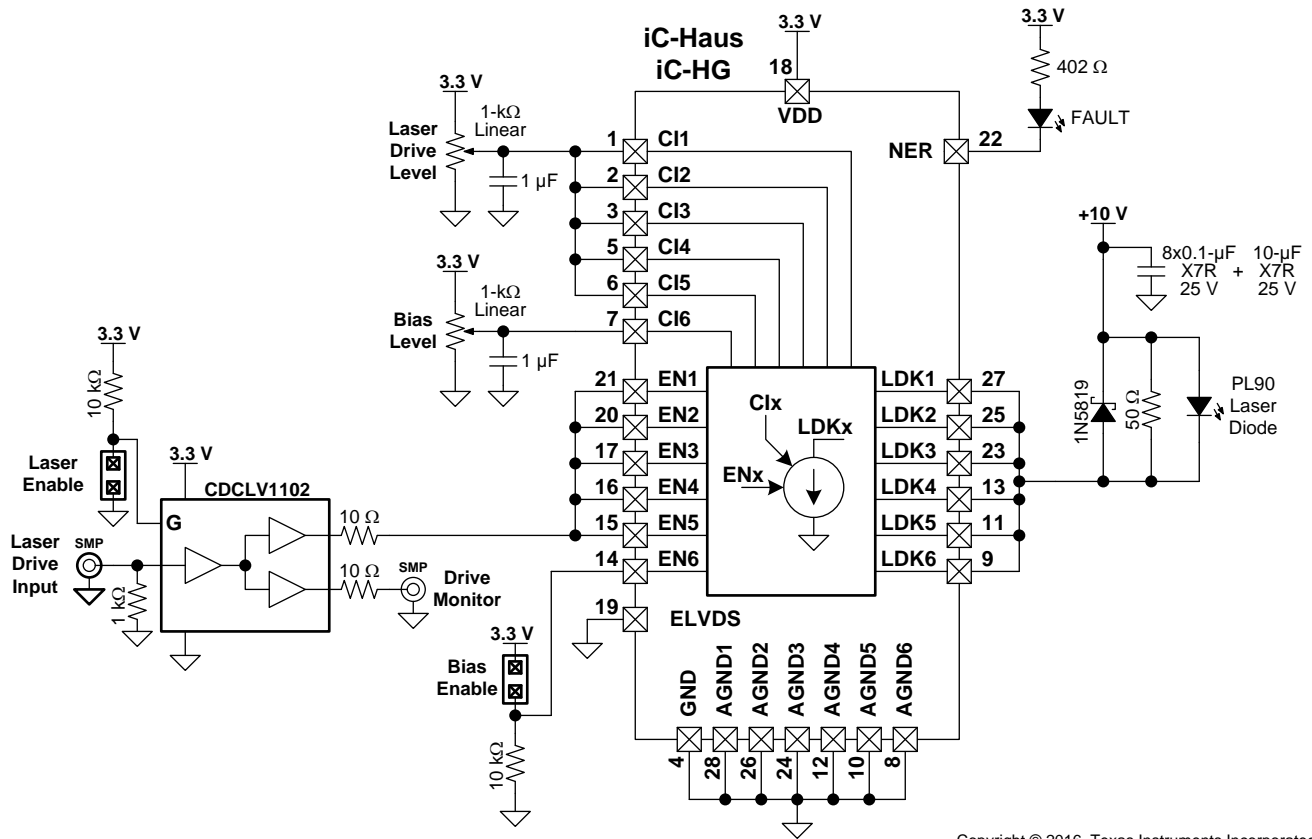
The DAC5682Z produces a differential current output that must be filtered and converted into a single-ended voltage before driving the laser. The circuit that 图 16 shows is composed of a passive termination and a 200-MHz low-pass filtering network that drives an OPA695 based, high-speed difference amplifier. To produce a $3\text{-}V_{pk}$ output, the gain of the difference amplifier was increased by changing R86 and R94 from $499\ \Omega$ to $1499\ \Omega$.


图 16. DAC Driver Circuit

For more information on this circuit, refer to [TSW3070 High Speed DAC Demonstration EVM](#).

2.3.6.3 Laser Driver

The iC-HG laser driver IC from iC-Haus has six switchable, high-speed current sources capable of delivering up to 1.5 A_{pk} each (or 500-mA DC). The sink current level on the LDKx is proportional to the voltage on the Clx when ENx is asserted high (and zero when ENx is low). As [图 17](#) shows, the first five channels are connected in parallel and the sixth is reserved for optional DC biasing. Output current is set by adjusting the *Laser Drive Level* and *Bias Level* multi-turn potentiometers. A CDCLV1102 clock fan-out buffer is used to drive EN1-EN5 with a copy sent to the *Drive Monitor* output, which is useful for triggering an oscilloscope during alignment and focusing. A jumper is provided to control the enable of the driver through the clock fan-out buffer.



Copyright © 2016, Texas Instruments Incorporated

图 17. Laser Driver Circuit

The 10-V laser diode supply is bypassed by eight parallel 0.1-μF bypass capacitors close to the laser diode to provide the high dynamic current required to generate a short pulse. A Schottky diode and 50-Ω resistor are placed in parallel with the laser diode to prevent voltage spikes due to reverse recovery when the current has been turned off. The layout has been carefully arranged to minimize the loop area formed by the supply (including bypassing) laser diode, output, and ground.

This design does not require biasing of the laser diode, so the *Bias Enable* jumper has been removed, which disables the sixth current source. The *Laser Drive Level* is adjusted to produce 6-A current pulses, which equates to about 5.75 W of laser output power. The pulse parameters are set to keep the laser average power less than 1 mW.

2.3.7 Photodiode Receive Path

2.3.7.1 High-Speed Receive Signal Chain

图 18 显示了一个高速接收信号链的块图，该链测量激光发射的光和从目标返回的光。此测量允许系统计算激光发射和信号返回之间的时间差。对于参考通道，少量激光光照射其光电二极管，产生微弱电流，该电流由 OPA857 高速 TIA 放大。此放大信号随后由 THS4541 高速 FDA 进一步放大，在 ADC3244 EVM 上通过一对同轴电缆传输。在 EVM 上，差分信号驱动第二个单位增益 THS4541 FDA，然后经过滤波并由 ADC3244 捕获。

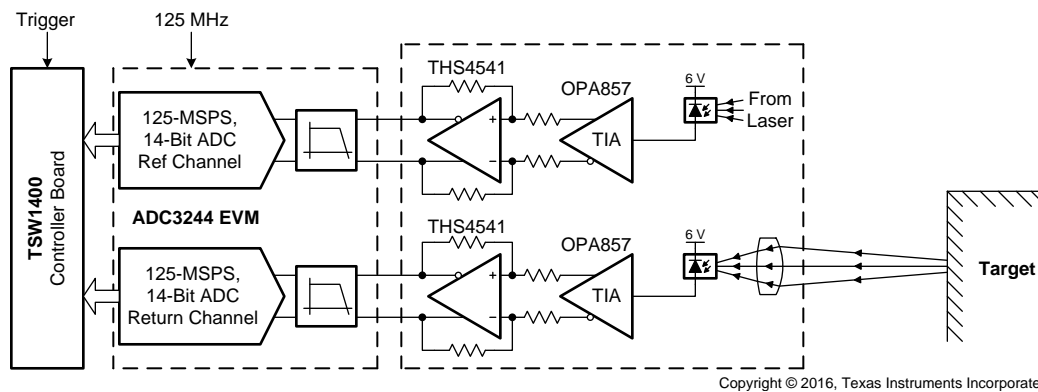


图 18. High-Speed Receive Signal Chain

返回通道与参考通道操作相同，但使用透镜聚焦从目标返回的光。请注意，如果接收电路位于 ADC 的同一电路板，则每个通道只需要一个 FDA。

2.3.7.2 Reference and Return Path TIAs

图 19 和图 20 分别显示了返回和参考通道 TIA 和 FDA 的块图。OSRAM SFH 2701 光电二极管通过 6-V 电源反向偏置，其阳极连接到 OPA857 TIA 的输入。当光照射光电二极管的活性区域时，会产生微小电流，该电流由 OPA857 器件转换为电压。安装增益选择跳线会降低增益，方法是并联 5-k Ω 和 20-k Ω 反馈电阻。TIA 的输出及其中点参考连接到 THS4541 器件，配置为差分增益为 5 且输出共模设置为 3.3-V 电源的一半。THS4541 器件的差分输出通过 50- Ω 源端匹配驱动 SMP 同轴连接器。

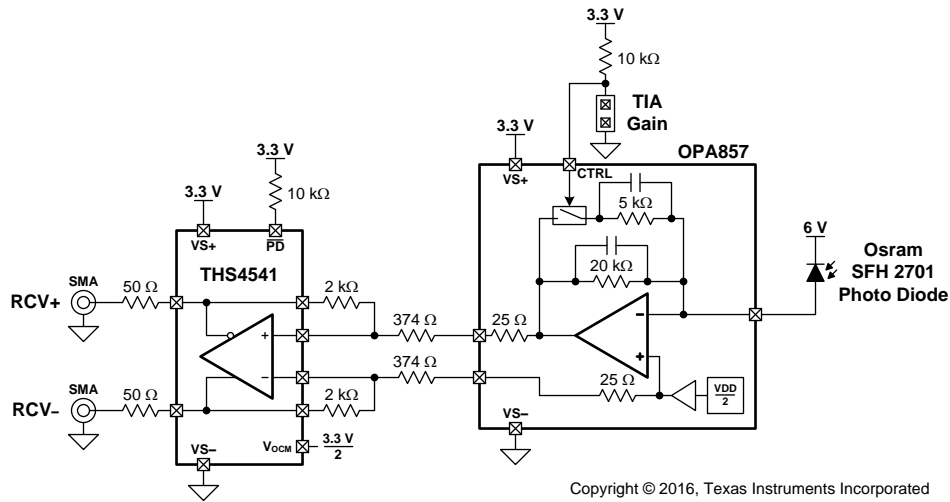


图 19. Return Path TIA

The reference path photodiode experiences a higher optical level than the return path, so the TIA gain is reduced by adding external resistors between the output and input. The TIA gain control is grounded to put the internal 5 kΩ in parallel with the 20-kΩ resistors. This implementation gives an approximate feedback resistance of 1.33 kΩ. The feedback resistance is split in half to reduce the parasitic capacitance experienced by both the output and input. The 0.1-pF capacitors are added to reduce the peaking at high frequencies.

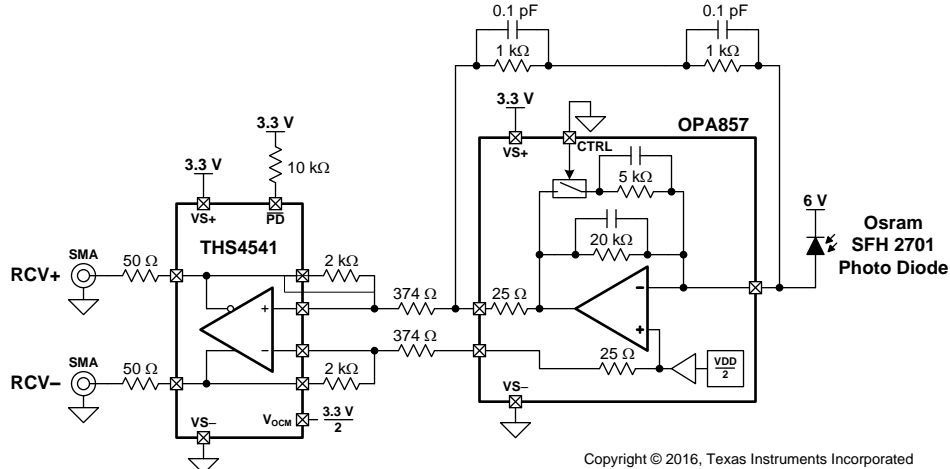
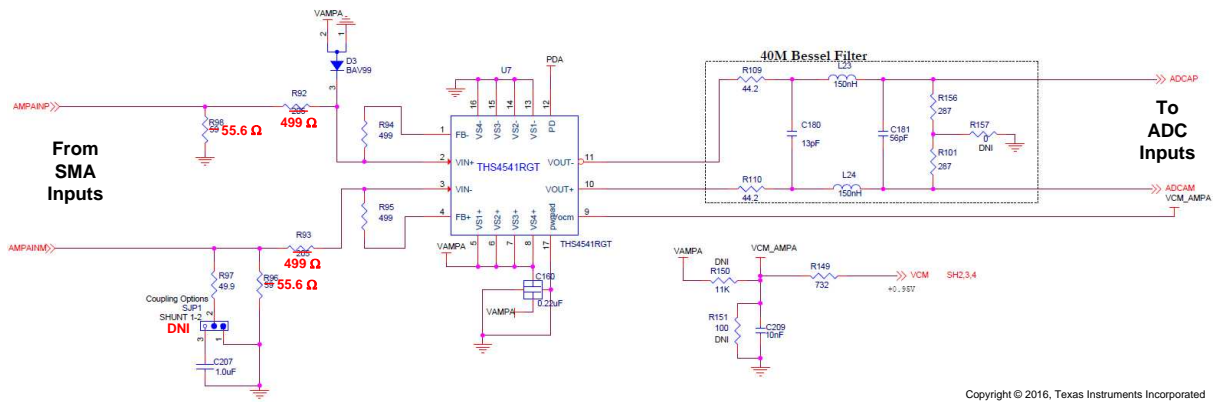


图 20. Reference Path TIA

For more information on this circuit, refer to the [Reference Design for Extending OPA857 Transimpedance Bandwidth \[2\]](#).

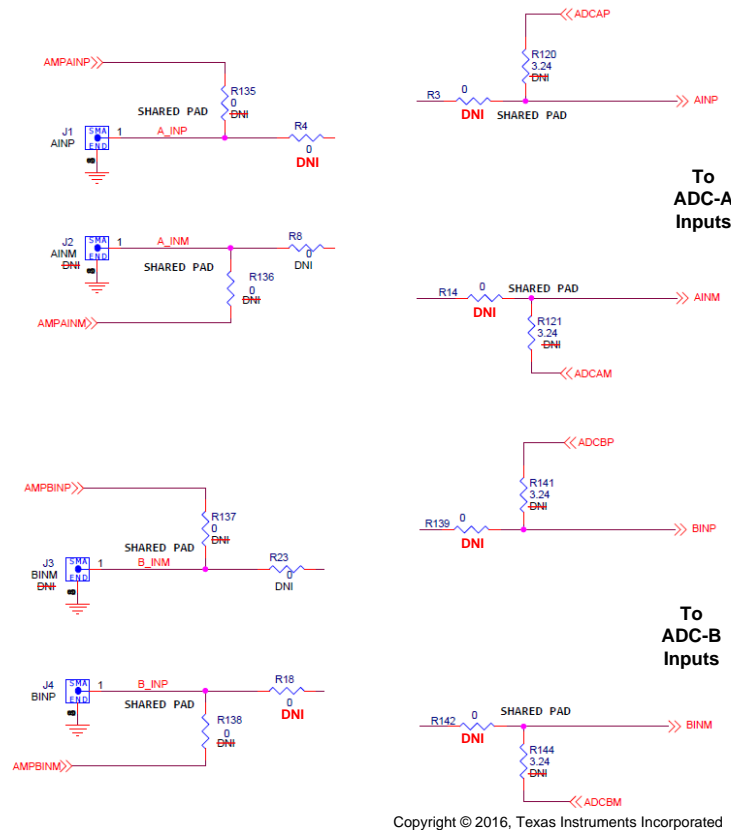
2.3.7.3 ADC Antialiasing and Driver Amplifier

The ADC3244 EVM has options for a transformer-coupled path and DC-coupled path. For this design, the DC-coupled path has been selected (see 图 21), which contains a THDS4541 FDA and 40-MHz Bessel low-pass filter. To select the DC-coupled path, remove R3, R4, R14, R18, R139, and R142 then populate R120, R121, R135 through R138, R141, and R144 with 0-Ω resistors (see 图 21).



Copyright © 2016, Texas Instruments Incorporated

图 21. ADC Antialiasing and Driver Amplifier



Copyright © 2016, Texas Instruments Incorporated

图 22. Selecting DC-Coupled Path on ADC3244 EVM

A differential input has been used, so the SJP1 and SJP2 soldered jumpers are removed and end launch SMAs J2 and J3 are installed. The THS4541s differential gain has also been reduced from 2 to 1 by changing R92, R93, R127, and R128 from 205 Ω to 499 Ω and R98, R96, R133, and R131 from 59.0 Ω to 55.6 Ω . For more information on this board, refer to the [ADC3244 Evaluation Module](#).

3 Testing and Results

3.1 Setup

Range measurements were taken in a laboratory setup with the optical driver and receiver board held stationary using a Thorlabs optical breadboard and pedestal mount as 图 23 shows . Several sheets of white printer paper attached to a stand were used as the target, which is both highly reflective and diffusive. The target was held perpendicular to the lab bench at a constant distance from the edge of the bench such that the range could be adjusted using a tape measure affixed to the bench. Adjustment of the optical breadboard was made such that the beam fired along the axis of the tape measure parallel to the lab bench (that is, at a constant height from the lab bench surface). An oscilloscope was used during the alignment and focusing process.

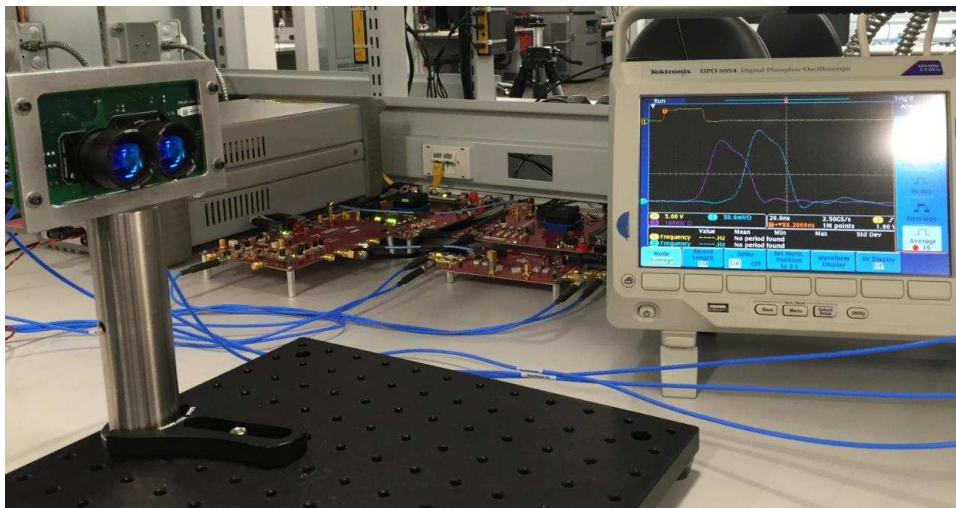


图 23. Laser Range Measurement Setup

3.2 Loading and Running DAC Waveform

The DAC5682Z GUI is used to configure the settings such that the DAC can operate with its PLL bypassed and with no interpolation. The GUI is also used to configure the CDCM7005 as a clock divider for the various clocks in the system. 图 24 shows the settings required to achieve this with the DAC.

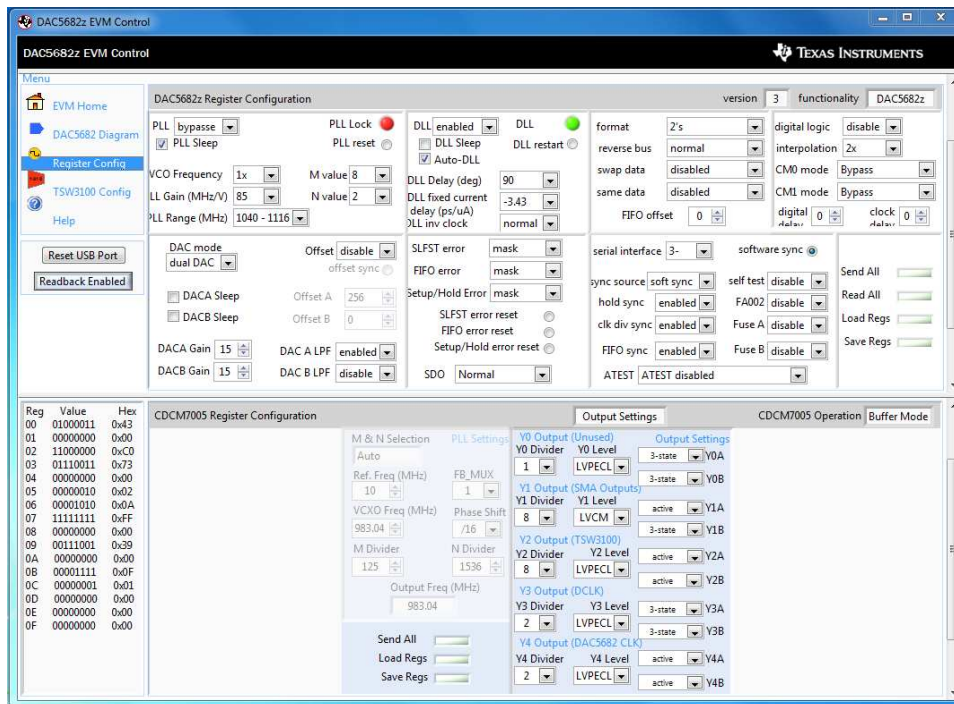


图 24. DAC5682Z GUI

When the DAC has been configured, HSDC Pro is used to load and run the laser stimulus waveform. 图 25 shows the loaded waveform in HSDC Pro. The DAC5682Z setting is selected and then *Data Rate* is set to 500 MSPS with a 2's complement data format. Finally, the stimulus file is loaded using the *Load External File* button. Clicking the *Send* button loads the waveform and starts the playback of the waveform.

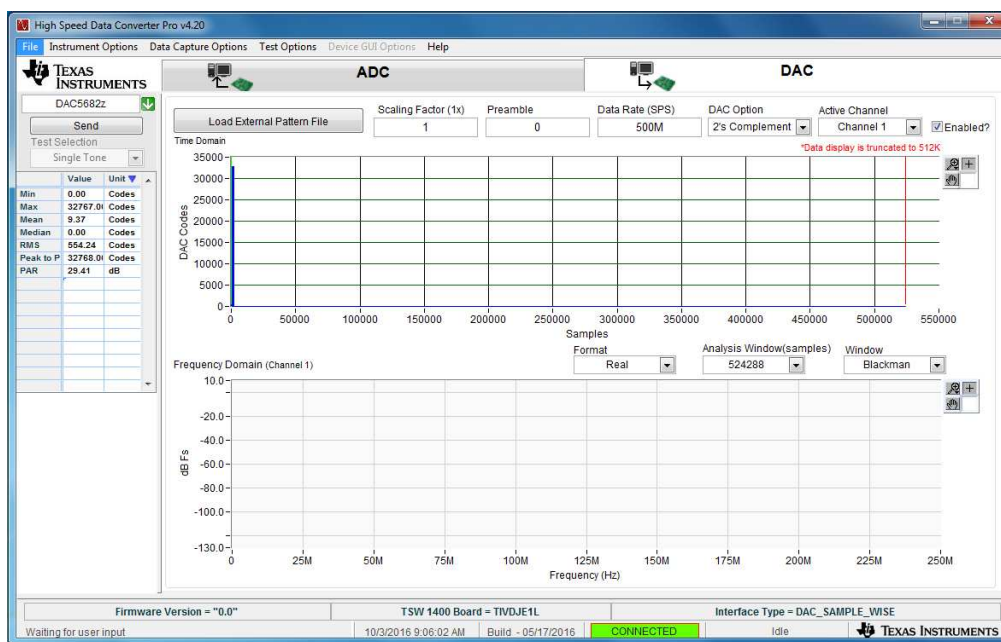


图 25. Loading DAC Waveform With HSDC Pro

3.3 Optical Alignment, Collimation and Focusing

When the DAC has been configured to generate the stimulus waveform, the laser must first be collimated and then aligned. Collimation is accomplished by adjusting the distance between the laser diode emitter and the collimating lens using the threads on the adjustable lens tube. As 图 26 shows, a Thorlabs VRC4 detector card was used to make the 905-nm light from the laser visible. The lens tube was adjusted until the spot produced had a bright rectangular shape that had a minimal increase in size as the card was moved away from the emitter.



图 26. Oscilloscope Capture of Reference and Return Signal

To align the laser, the flange-mounting screws were loosened such that the flange position is adjustable. The detector card was placed at a range of approximately 2 m and the flange position was adjusted until the center of the beam was located in a position on axis with the emitter. Alignment was further refined as range was increased such that movement of the center of the laser spot on the card was minimized. The mounting screws were then tightened to lock the alignment of the laser.

Alignment and focusing of the receiver lens was accomplished in a similar fashion as collimation. An oscilloscope, triggered by the pulse monitor output of the driver and receiver board, was used to monitor the output of the received return pulse during adjustment, as 图 27 shows. An iterative process of adjusting alignment and focus was repeated until the strongest return signal could be obtained at 5 m.

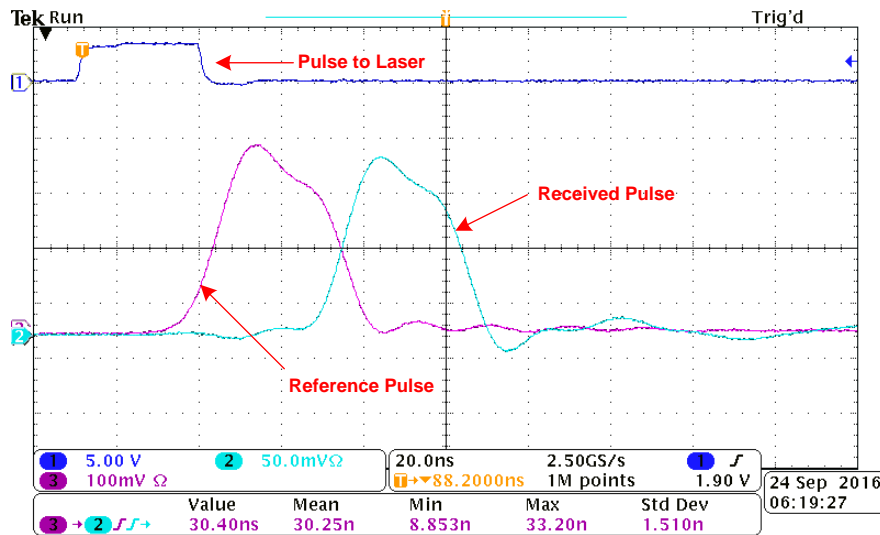


图 27. Oscilloscope Capture of Reference and Return Signal

3.4 Configuring ADC and Capturing ADC Results

After powering up the ADC3244 EVM, the reset button on the board must be pressed to reset the ADC. The GUI can then be launched where the dither and chopper functions are disabled by checking the four boxes as 图 28 shows.

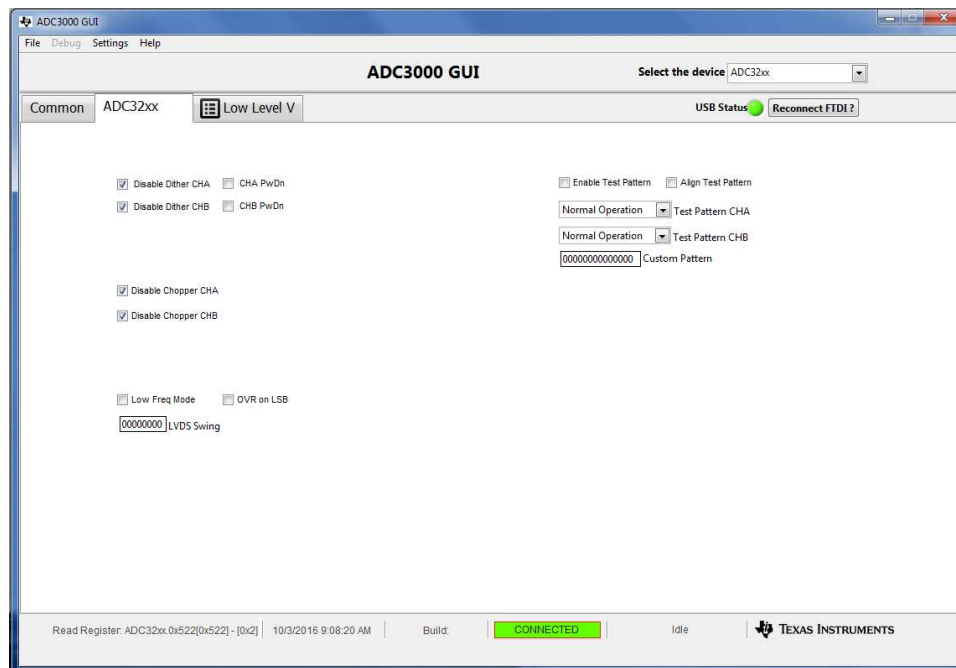


图 28. ADC3244 GUI

Next, the HSDC Pro software is launched, which connects to the TSW1400 controller board. The *ADC324x_2W_14bit* device is selected with the *ADC Output Rate* set to 125 MHz. Triggering is enabled by clicking the *Trigger mode enable* check box in the *Trigger Option* menu under *Data Capture Options* (see 图 29). Because of the low refresh rate, only one frame is captured during each acquisition.

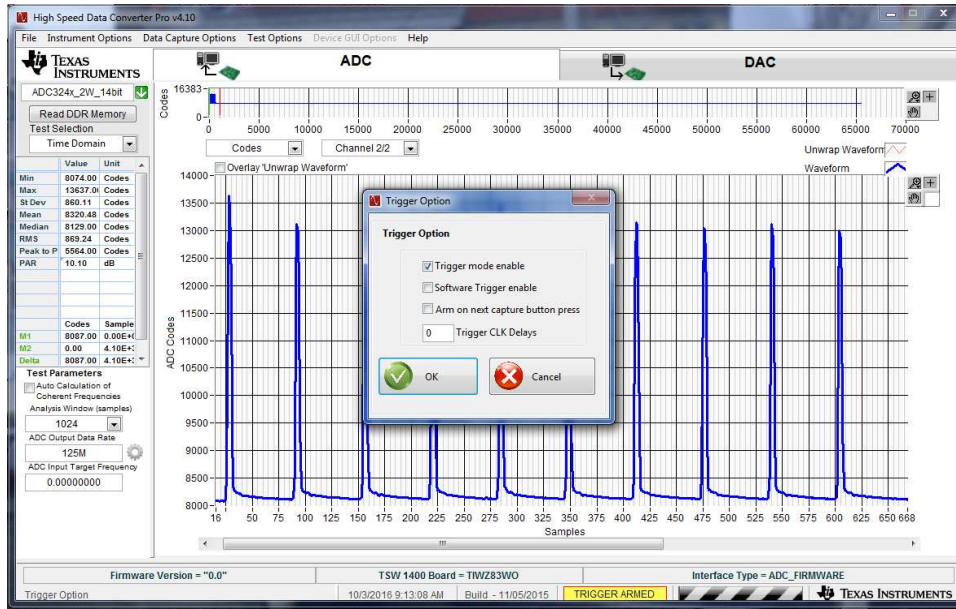


图 29. Trigger Setup

图 30 和 图 31 显示参考信号和返回信号的捕获，分别。

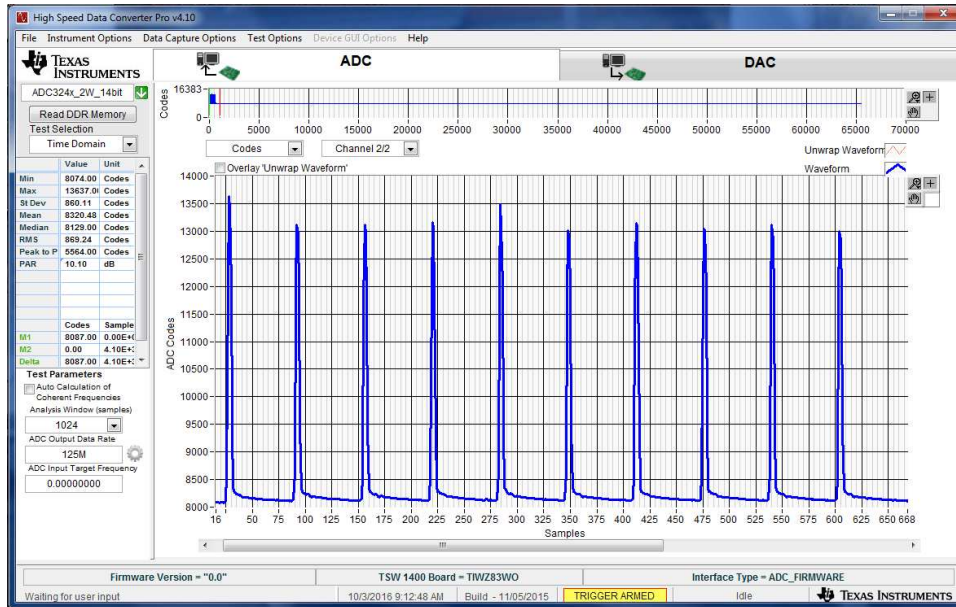


图 30. Captured Reference Signal

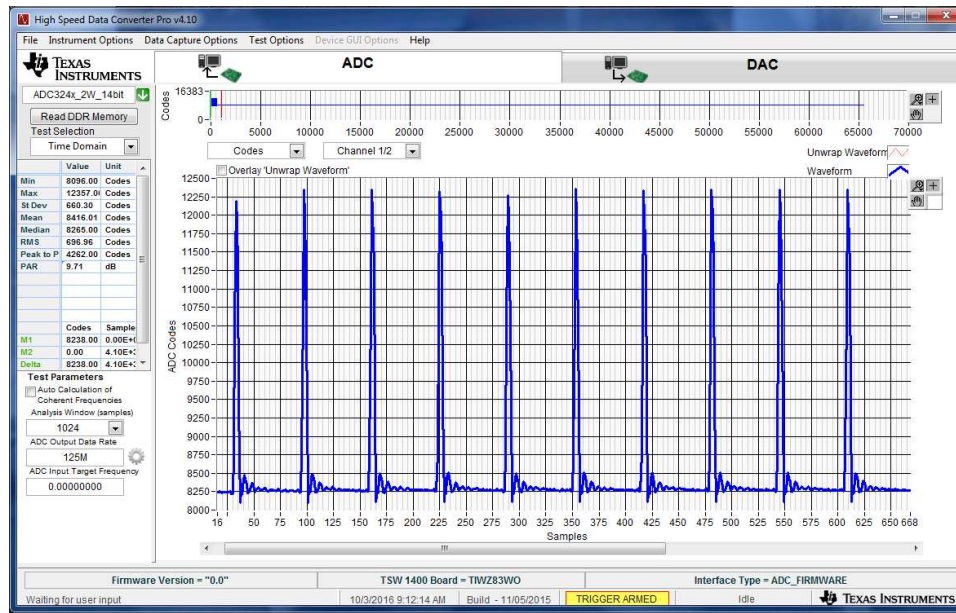


图 31. Captured Return Signal

Each capture was saved and processed to calculate range.

3.5 Range Results

Distance was measured from 1.5 m to 9 m using a white printer paper target with the laser adjusted to produce $\approx 5.75\text{-W}$ pulses. Each frame was composed of ten 30-ns pulses spaced 512 ns apart. A 2-ms frame rate was selected to keep the average power under 1 mW. 128 frames were collected at each distance where range mean and standard deviation were calculated after correcting for gain and offset. [图 32](#) shows the resulting measured range versus range.

The lower TIA gain setting was used from 1.5 m to 3 m and the higher setting was used from 3 m to 9 m. During initial data collection, it was determined that the ADC EVMs 40-MHz Bessel filter did not have sufficient attenuation at the Nyquist and beyond, which caused degradation in the range mean and standard deviation performance due to aliasing. Mini-Circuits LPF-BP50+ filters were installed on each ADC input, which eliminated this issue. A steeper filter response, such as a Chebychev, is also sufficient in this application for solving this problem.

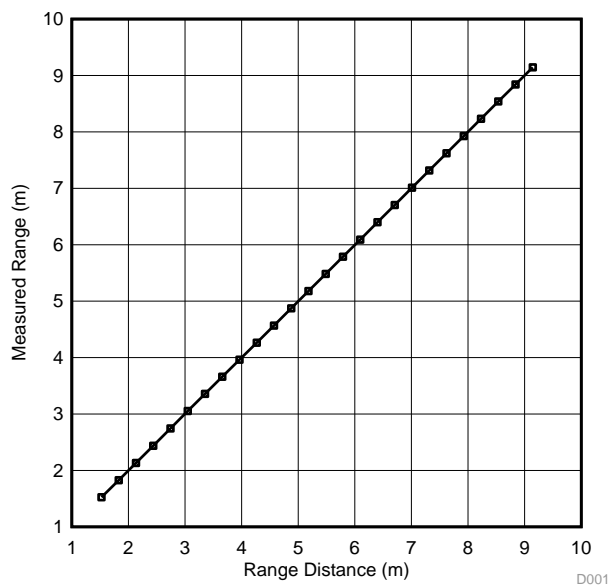


图 32. Measured Range versus Range

图 33 shows the standard deviation of the measured mean of the range versus range. The dip at 3 m was the result of the increase of the TIAs gain, which reduced the input-referred noise floor. The increase of standard deviation with range can be directly attributed to the reduction in the signal-to-noise ratio (SNR), which is the result of the received amplitude decreasing proportionally to the square of range.

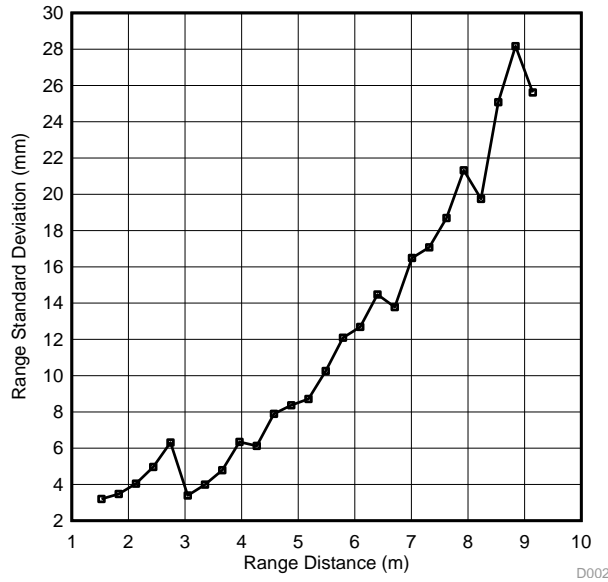


图 33. Range Standard Deviation versus Range

图 34 shows the range error in the mean versus range. This error can be attributed to a number of factors including the precision of the measurement setup, crosstalk between the driver and receiver, and residual aliasing in the ADC path. The maximum range error of 5.5 mm corresponds to a time error of ± 37 ps, which demonstrates that even with a 125-MSPS ADC, time estimates substantially less than the sample period can be estimated.

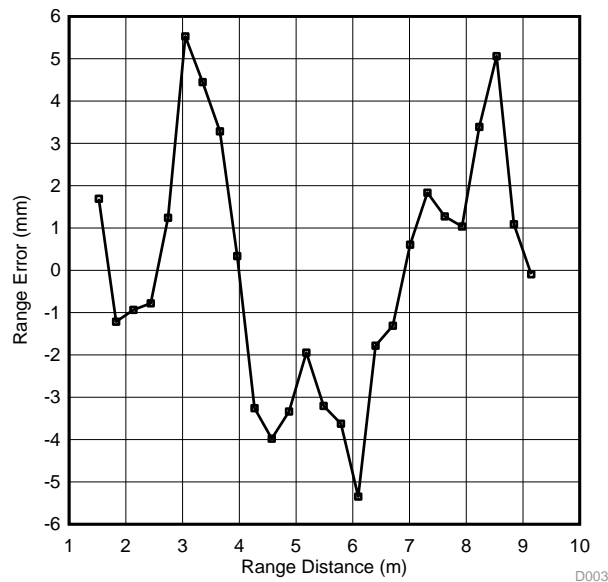


图 34. Range Error versus Range

图 35 compares the attenuation versus range for white printer paper, brown cardboard, black powder coated steel and Thorlabs black optical masking tape. Attenuation is shown relative to the level received with the white printer paper at 2.13 m. This relation shows that the received signal attenuation is proportional to the square of distance for diffusive materials regardless of the reflection coefficient. This amplitude information provides information useful in target detection because the amplitude at a given range is known for each type of material.

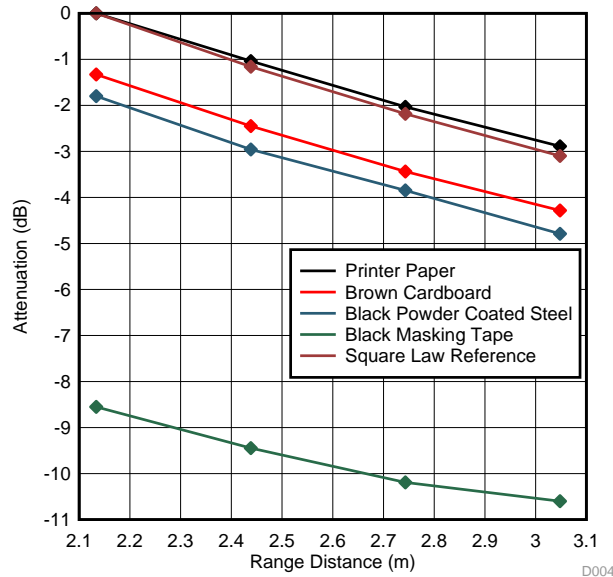


图 35. Attenuation versus Range

4 Design Files

4.1 Schematics

To download the schematics, see the design files at [TIDA-001187](#).

4.2 Bill of Materials

To download the bill of materials (BOM), see the design files at [TIDA-001187](#).

4.3 PCB Layout Recommendations

4.3.1 Layout Prints

To download the layer plots, see the design files at [TIDA-001187](#).

4.4 Cadence Project

To download the Cadence project files, see the design files at [TIDA-001187](#).

4.5 Gerber Files

To download the Gerber files, see the design files at [TIDA-001187](#).

4.6 Assembly Drawings

To download the assembly drawings, see the design files at [TIDA-001187](#).

5 Software Files

To download the software files, see the design files at [TIDA-001187](#).

6 Related Documentation

1. Texas Instruments, [TSW3070EVM: Amplifier Interface to Current Sink DAC - Arbitrary Waveform Generator Demonstration](#), User's Guide (SLWU055A)
2. Texas Instruments, [Reference Design for Extending Transimpedance Bandwidth of OPA857](#), User's Guide (TIDUC73)

7 About the Author

DAVE GUIDRY is a member of the applications team in the high speed catalog converters group at Texas Instruments. He received his BSEE from Texas A&M University, College Station in 2001. Since graduation he has worked for Texas Instrument with roles in SOC characterization, production test development, test strategy, instrumentation design, analog IC design, systems and applications. Mr. Guidry is a Senior Member of TI's technical staff.

修订版本 B 历史记录

注：之前版本的页码可能与当前版本有所不同。

Changes from A Revision (February 2017) to B Revision	Page
• 已更改 将测量距离规格从“1.5m 至 9m”更改为“高达 9m 或更远”.....	1
• 已添加 在“特性”中添加了“为选定的器件提供了汽车级版本”.....	1
• 已添加 在“应用”中添加了“汽车扫描 LIDAR 和无人机”.....	1
• Reorganized order of sections; no changes to content	2
• 已添加 content to System Description section: "The optics used in this design are optimized for up to 9 m of distance. A longer range is possible through a choice of optics.".....	3

修订版本 A 历史记录

Changes from Original (November 2016) to A Revision	Page
• 已更改 将标题从“使用脉冲飞行时间的光学距离测量参考设计”更改为“使用高速数据转换器的 LIDAR 脉冲飞行时间参考设计”.....	1

有关 TI 设计信息和资源的重要通知

德州仪器 (TI) 公司提供的技术、应用或其他设计建议、服务或信息，包括但不限于与评估模块有关的参考设计和材料（总称“TI 资源”），旨在帮助设计人员开发整合了 TI 产品的应用；如果您（个人，或如果是代表贵公司，则为贵公司）以任何方式下载、访问或使用了任何特定的 TI 资源，即表示贵方同意仅为该等目标，按照本通知的条款进行使用。

TI 所提供的 TI 资源，并未扩大或以其他方式修改 TI 对 TI 产品的公开适用的质保及质保免责声明；也未导致 TI 承担任何额外的义务或责任。TI 有权对其 TI 资源进行纠正、增强、改进和其他修改。

您理解并同意，在设计应用时应自行实施独立的分析、评价和判断，且应全权负责并确保应用的安全性，以及您的应用（包括应用中使用的 TI 产品）应符合所有适用的法律法规及其他相关要求。您就您的应用声明，您具备制订和实施下列保障措施所需的一切必要专业知识，能够 (1) 预见故障的危险后果，(2) 监视故障及其后果，以及 (3) 降低可能导致危险的故障几率并采取适当措施。您同意，在使用或分发包含 TI 产品的任何应用前，您将彻底测试该等应用和该等应用所用 TI 产品的功能。除特定 TI 资源的公开文档中明确列出的测试外，TI 未进行任何其他测试。

您只有在为开发包含该等 TI 资源所列 TI 产品的应用时，才被授权使用、复制和修改任何相关单项 TI 资源。但并未依据禁止反言原则或其他法律授予您任何 TI 知识产权的任何其他明示或默示的许可，也未授予您 TI 或第三方的任何技术或知识产权的许可，该等产权包括但不限于任何专利权、版权、屏蔽作品权或与使用 TI 产品或服务的任何整合、机器制作、流程相关的其他知识产权。涉及或参考了第三方产品或服务的信息不构成使用此类产品或服务的许可或与其相关的保证或认可。使用 TI 资源可能需要您向第三方获得对该等第三方专利或其他知识产权的许可。

TI 资源系“按原样”提供。TI 兹免除对 TI 资源及其使用作出所有其他明确或默示的保证或陈述，包括但不限于对准确性或完整性、产权保证、无复发故障保证，以及适销性、适合特定用途和不侵犯任何第三方知识产权的任何默认保证。

TI 不负责任何申索，包括但不限于因组合产品所致或与之有关的申索，也不为您辩护或赔偿，即使该等产品组合已列于 TI 资源或其他地方。对因 TI 资源或其使用引起或与之有关的任何实际的、直接的、特殊的、附带的、间接的、惩罚性的、偶发的、从属或惩戒性损害赔偿，不管 TI 是否获悉可能会产生上述损害赔偿，TI 概不负责。

您同意向 TI 及其代表全额赔偿因您不遵守本通知条款和条件而引起的任何损害、费用、损失和/或责任。

本通知适用于 TI 资源。另有其他条款适用于某些类型的材料、TI 产品和服务的使用和采购。这些条款包括但不限于适用于 TI 的半导体产品 (<http://www.ti.com/sc/docs/stdterms.htm>)、[评估模块](http://www.ti.com/sc/docs/sampters.htm)和样品 (<http://www.ti.com/sc/docs/sampters.htm>) 的标准条款。

邮寄地址：上海市浦东新区世纪大道 1568 号中建大厦 32 楼，邮政编码：200122
Copyright © 2017 德州仪器半导体技术（上海）有限公司